Pharm Res (2012) 29:3169–3179
DOI 10.1007/s11095-012-0812-7

RESEARCH PAPER

Prevention of Orthopedic Device-Associated Osteomyelitis Using Oxacillin-Containing Biomineral-Binding Liposomes

Xin-Ming Liu • Yijia Zhang • Fu Chen • Irine Khutsishvili • Edward V. Fehringer • Luis A. Marky • Kenneth W. Bayles • Dong Wang

Received: 12 March 2012 / Accepted: 21 May 2012 / Published online: 26 June 2012

ABSTRACT

Purpose To develop novel biomineral-binding liposomes (BBL) for the prevention of orthopedic implant associated osteomyelitis.

Methods A biomineral-binding lipid, alendronate-tri(ethyleneglycol)-cholesterol conjugate (ALN-TEG-Chol), was synthesized through Cu(I)-catalyzed Huisgen 1,3-dipolar cycloaddition (a versatile click reaction). Mixing with other excipients, the new lipid was used to develop BBL. Thermodynamic behavior was studied by differential scanning calorimetry (DSC). *In vitro* biomineral-binding potential and kinetics were evaluated on hydroxyapatite (HA, a widely used material for orthopedic implant devices) particles. Oxacillin was encapsulated into BBL and used for *in vitro* evaluation in preventing *Staphylococcus aureus* biofilm formation.

Results DSC analysis showed that ALN-TEG-Chol could inhibit the phase transition of liposomes by reducing its cooperativity, yielding liposomes with thermodynamic stability similar to liposomes containing regular cholesterol. BBL showed fast and strong binding ability to HA. Oxacillin-loading BBL demonstrated significantly better preventive efficacy against bacteria colonization when challenged with *S. aureus* isolate, implying its potential in preventing orthopedic implant associated osteomyelitis.

Conclusions In this proof of concept study, novel BBL has been successfully developed and validated for reducing the frequency of implantable device-related infections.

KEY WORDS bisphosphonates · liposomes · orthopaedic implant · osteomyelitis · oxacillin

INTRODUCTION

Osteomyelitis or bone infection, caused by bacteria contamination at the time of trauma, surgery, orthopedic device implantation, or direct colonization/systemic transmission represents a substantial challenge world-wide for clinical orthopedic practice (1). For orthopedic trauma, up to 60% of open fractures are contaminated with bacteria at the time of injury (2), which leads to significant risk of infection (5–33%) (3–6). Postoperative osteomyelitis is another important problem in orthopedic practice (7). Despite the widespread prophylactic use of antibiotic and the enhanced aseptic operative training, post-arthroplasty infection, for example, still occurs in 1.2% of primary arthroplasties and 3–5% of revisions (8,9). These complications often result in prolonged hospitalization, high patient care expense and significantly worse treatment outcomes.

Osteomyelitis has been generally considered as one of the most difficult orthopedic complications to be treated clinically (10). Due to the presence of antibiotic-resistant bacteria and the

Xin-Ming Liu and Yijia Zhang contributed equally to this work.

X.-M. Liu • Y. Zhang • F. Chen • I. Khutsishvili • L. A. Marky • D. Wang (✉)
Department of Pharmaceutical Sciences
University of Nebraska Medical Center
986025 Nebraska Medical Center, COP 3026
Omaha, NE 68198-6025, USA
e-mail: dwang@unmc.edu

E. V. Fehringer
Department of Orthopaedic Surgery and Rehabilitation
University of Nebraska Medical Center
981080 Nebraska Medical Center
Omaha, Nebraska 68198-1080, USA

K. W. Bayles
Department of Pathology and Microbiology
University of Nebraska Medical Center
983135 Nebraska Medical Center
Omaha, Nebraska 68198-3135, USA

Present Address:
X.-M. Liu
Department of Pharmacology and Experimental Neurosciences
Durham Research Center 3046
University of Nebraska Medical Center
985800 Nebraska Medical Center
Omaha, Nebraska 68198-5800, USA

formation of biofilms at the site of chronic infection, maintenance of very high antimicrobial level at the infection sites is needed to completely eradicate the pathogens. The anatomical feature of the relatively limited blood supply to the hard tissue (1,11) and the lack of osteotropicity among the commercially available antimicrobials make the clinical management of osteomyelitis very challenging. Clinically, high systemic doses of antimicrobials have been used to facilitate sufficient tissue and biofilm penetration at the infection sites. Such strategy is not preferable due to the potential of serious systemic toxicities (1). Repeated implantations of antimicrobial loaded delivery devices have also been used to maintain the local drug concentration with limited benefit (12). To improve the biomineral specificity of the antimicrobials and maintenance of their effective local concentration, several osteotropic antimicrobial prodrugs have been developed, but are yet to be validated *in vivo* for their therapeutic efficacy. Early results suggest a marginal benefit in improving the efficacy of the antimicrobial activity (13,14).

Recognizing these challenges, we believe the best window of opportunity for preventing bacterial infection is at the time of injury or initial surgery when the colonization is still very limited. Taking orthopedic implantation for example, initial loading of the device surface with antimicrobials (which does not have to be at very high level) would prevent any bacteria from colonizing at the bone/implant interface. To incorporate antimicrobials to the implant surface, orthopedic devices with antimicrobial-containing polymer coatings have been developed using different methodologies, with their clinical efficacy and safety yet to be defined (15,16).

In this manuscript, we propose a novel strategy to address the orthopedic device-associated osteomyelitis. At the center of our design is a biomineral/metal binding liposome system, which could be used to encapsulate various antimicrobials and quickly load them onto an implant surface. Not only will this system avoid some potential limitations of the current approaches, but due to its fast loading kinetics (within a few minutes) it will also offer the orthopedic surgeons significant flexibility in the operating room (OR) with the ability to load the device with selected combination of antimicrobials and other therapeutic agents for more personalized prophylaxis.

Many orthopedic implants have a hydroxyapatite (HA) coating to promote the osteointegration of the devices. To allow loading onto such implant surfaces, we designed and synthesized an alendronate-tri(ethyleneglycol)-cholesterol conjugate (ALN-TEG-Chol) through a versatile "click" reaction (17) (Fig. 1). When inserted into the lipid bilayer, this molecular design affords a biomineral-binding liposomal delivery platform, which by anchoring to the HA surface and gradually releasing its antimicrobial content would provide a therapeutic barrier to prevent bacterial colonization on the device (Fig. 2). The same concept can be easily

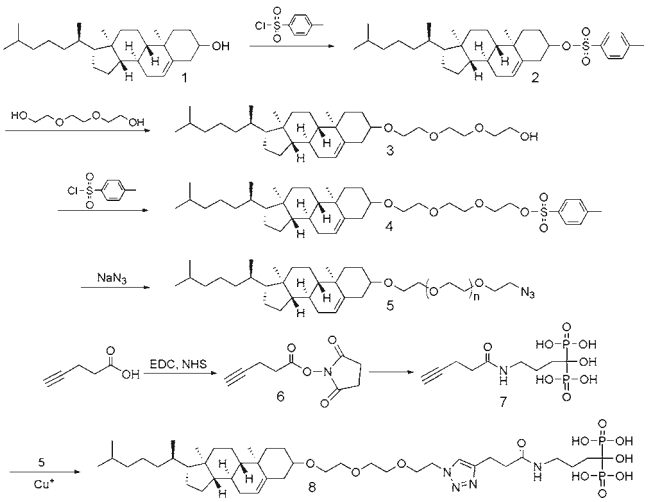

Fig. 1 Synthesis of biomineral-binding lipid ALN-TEG-Chol.

extrapolated to other implant surfaces (e.g. titanium, stainless steel, etc.) as specific binding moieties to these surfaces have been developed (18,19). Since *Staphylococcus aureus* is one of the major causes of device-associated osteomyelitis (20), oxacillin (a penicillinase-resistant β-lactam antibiotics) was chosen as a model drug in this proof of principle evaluation to test the *in vitro* efficacy of the liposomal platform in preventing *S. aureus* biofilm formation.

MATERIALS AND METHODS

Materials

Alendronate (ALN) was purchased from Ultratech India Ltd. (New Mumbai, India). Pentynoic acid 2,5-dioxo-

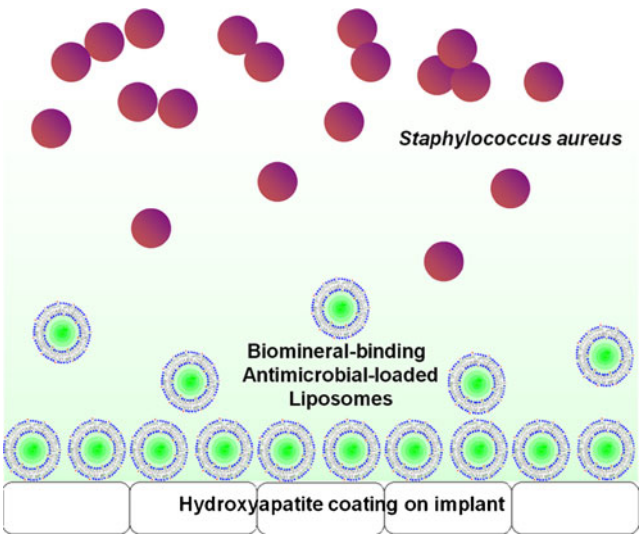

Fig. 2 Hypothetical working mechanism of biomineral-binding liposomes on hydroxyapatite (HA)-coated orthopedic implant surface.

pyrrolidin-1-yl ester (compound 6 in Fig. 1) and 1-hydroxy-4-pent-4-ynamidobutane-1,1-diyldiphosphonic acid (compound 7 in Fig. 1) were synthesized as described previously (21). Tris-(hydroxypropyltriazolylmethyl)amine (THPTA, stabilizing agent in "click" reaction) was synthesized as described previously (22). Oxacillin sodium salt, L-α-phosphatidylcholine (LPC) was obtained from Sigma-Aldrich Co. (St. Louis, MO). 1,2-Distearoyl-sn-glycero-3-phosphocholine (DSPC) was purchased from NOF America (White Plains, NY). Cholesterol (compound 1 in Fig. 1) was purchased from Alfa Aesar (Ward Hill, MA). Triethylene glycol was obtained from TCI America (Portland, OR). Hydroxyapatite particles (HA, DNA grade Bio-Gel HTP gel) were purchased from Bio-Rad (Hercules, CA). HA discs (0.5′ diameter × 0.04–0.06′ thick) were purchased from Clarkson Chromatography Products, Inc. (South Williamsport, PA). PD-10 columns (Sephadex G-25 M) were purchased from GE Healthcare (Piscataway, NJ). Dialysis membrane with molecular weight cutoff (MWCO) size of 25 kDa of globular protein was purchased from Spectrum Laboratories (RanchoDominguez, CA). All other reagents and solvents, if not specified, were purchased from either Fisher Scientific (Pittsburgh, PA) or Acros Organics (Morris Plains, NJ).

Methods

NMR spectra were recorded on a Varian Inova Unity 500 NMR Spectrometer. The thermodynamic behavior of liposomes was studied by Microcal VP-DSC differential scanning microcalorimeter (Northampton, MA). Liposome size, size distribution, and charge were measured on a dynamic light scattering (DLS) ZetaPlus analyzer (Brookhaven Instrument Co.) equipped with a Multiangle Sizing Option (BI-MAS). An Agilent 1100 HPLC system with a quaternary pump (with degasser), an autosampler and a diode-array based UV detector was used for oxacillin concentration analysis. An Olympus BX51 microscope with an X-Cite® 120Q fluorescence microscopy illumination system was utilized for the binding potential study.

Synthesis of Cholest-5-en-3β-yloxy-tosylate (Tos-Chol; compound 2)

To an ice-cooled solution of cholesterol (compound 1, 1.933 g, 5 mmol) and triethylamine (1.125 mL, 7.5 mmol) in 40 mL dry dichloromethane (DCM), *p*-toluenesulfonylchloride (1.43 g, 7.5 mmol) was slowly added at 0°C with 4-dimethylaminopyridine (DMAP, 60 mg, 0.5 mmol) as the catalyst. The reaction mixture was then allowed to stir at room temperature overnight. The reaction mixture was washed with 1 N HCl (2×40 mL), and brine (2×40 mL); the organic layer was separated, dried over anhydrous Na_2SO_4, and evaporated under vacuum. The resulting crude product was purified with silica gel chromatography (Hexane/Chloroform 4:1). Yield: 60%. ^{1}H NMR ($CDCl_3$, 500 MHz) δ (ppm) 7.80 (d, 2H, J=7.8 Hz), 7.33 (d, 2H, J=8.3 Hz), 5.30 (d, 1H, J=4.9 Hz), 4.34–4.30 (m, 1H), 2.44 (s, 3H), 2.44–2.41 (m, 1H), 2.28–2.25 (m, 1H), 2.00–0.98 (m, 26H), 0.96 (s, 3H), 0.90 (d, 3H, J=6.3 Hz), 0.86 (dd, 6H, J_1=6.3 Hz, J_2=2.2 Hz), 0.65 (s, 3H); ^{13}C NMR ($CDCl_3$, 125 MHz) δ (ppm) 144.4, 138.8, 134.6, 129.7, 127.6, 123.5, 82.4, 56.6, 56.0, 49.9, 42.2, 39.6, 39.5, 38.8, 36.8, 36.3, 36.1, 35.7, 31.8, 31.7, 28.6, 28.2, 28.0, 24.2, 23.8, 22.8, 22.5, 21.6, 20.9, 19.1, 18.7, 11.8.

Synthesis of 8-(cholest-5-en-3β-yloxy)-3,6-dioxaoctan-1-ol (TEG-Chol; compound 3)

To a solution of cholesteryl tosylate (2.16 g, 4 mmol) in dry 1,4-dioxane (30 mL) was added tri(ethyleneglycol) (15 mL, 111 mmol). The reaction mixture was refluxed for about 6 h under an argon atmosphere (TLC to confirm the end of the reaction). After evaporating 1,4-dioxane, the reaction mixture was dissolved in 50 mL chloroform, extracted with saturated $NaHCO_3$ aqueous solution (2×50 mL) and brine (2×50 mL), dried over anhydrous Na_2SO_4, and concentrated under vacuum to give crude product. The crude product was further purified with silica gel chromatography (Hexane/Ethyl acetate 2:1) as a white oily solid. Yield: 78.5%. ^{1}H NMR ($CDCl_3$, 500 MHz) δ (ppm) 5.34 (d, 1H, J=4.9 Hz), 3.76–3.60 (m, 12H), 3.21–3.16 (m, 1H), 2.79 (m, 1H), 2.39–2.36 (m, 1H), 2.24–2.19 (m, 1H), 2.05–1.01 (m, 25H), 0.99 (s, 3H), 0.91 (d, 3H, J=6.3 Hz), 0.86 (dd, 6H, J_1=6.3 Hz, J_2=2.2 Hz), 0.67 (s, 3H); ^{13}C NMR ($CDCl_3$, 125 MHz) δ (ppm) 140.8, 121.5, 79.5, 72.6, 70.8, 70.5, 70.3, 67.1, 61.6, 56.7, 56.1, 50.1, 42.2, 39.7, 39.4, 38.9, 37.1, 36.8, 36.1, 35.7, 31.9, 31.8, 28.2, 28.1, 27.9, 24.2, 23.7, 22.8, 22.5, 21.0, 19.3, 18.6, 11.8.

Synthesis of 8-(cholest-5-en-3β-yloxy)-3,6-dioxaoctanyl tosylate (Tos-TEG-Chol; compound 4)

To an ice-cooled solution of 8-(cholest-5-en-3β-yloxy)-3,6-dioxaoctan-1-ol (518 mg, 1 mmol) and triethyl amine (0.2 mL, 1.3 mmol) in 10 mL dry DCM, *p*-toluenesulfonylchloride (248 mg, 1.3 mmol) was slowly added at 0°C with DMAP (12 mg, 0.1 mmol) as the catalyst. After reacting at room temperature overnight, the reaction mixture was washed with 1 N HCl (2×10 mL), and brine (2×10 mL). The organic layer was separated, dried over anhydrous Na_2SO_4, and evaporated under vacuum. The crude product was further purified with silica gel chromatography (Hexane/Chloroform 4:1). Yield: 75%. ^{1}H NMR ($CDCl_3$, 500 MHz) δ (ppm) 7.80 (d, 2H, J=8.3 Hz), 7.34 (d, 2H, J=7.8 Hz), 5.34 (d, 1H, J=4.9 Hz), 4.16 (t, 2H, J=4.9 Hz),

3.69 (t, 2H, J=4.9 Hz), 3.61–3.59 (m, 8H), 3.18–3.15 (m, 1H), 2.45 (s, 3H), 2.37–2.34 (m, 1H), 2.22–2.19 (m, 1H), 2.02–1.01 (m, 26H), 0.99 (s, 3H), 0.91 (d, 3H, J=6.3 Hz), 0.86 (dd, 6H, J_1=6.3 Hz, J_2=2.2 Hz), 0.67 (s, 3H); ^{13}C NMR ($CDCl_3$, 125 MHz) δ (ppm) 144.7, 140.9, 132.9, 129.8, 127.9, 121.5, 79.4, 70.9, 70.7, 70.5, 69.2, 68.6, 67.2, 56.7, 56.1, 50.1, 42.3, 39.7, 39.5, 39.0, 37.2, 36.8, 36.1, 35.7, 31.9, 31.8, 28.3, 28.2, 28.0, 24.2, 23.8, 22.8, 22.5, 21.6, 21.0, 19.3, 18.7, 11.8.

Synthesis of 8-(cholest-5-en-3β-yloxy)-3,6-dioxaoctanyl azide (Azido-TEG-Chol; compound 5)

8-(Cholest-5-en-3β-yloxy)-3,6-dioxaoctanyl tosylate (337 mg, 0.5 mmol) was suspended in ethanol (5 mL), sodium azide (325 mg, 5 mmol) was then added. After reflux overnight and cooling to room temperature, the solution was concentrated and then dissolved in 10 mL of chloroform. The resulting mixture was washed with saturated $NaHCO_3$ aqueous solution (2×50 mL), brine (2×50 mL), dried over anhydrous Na_2SO_4, and concentrated under vacuum to give an oily product. Yield: 95%. ^{1}H NMR ($CDCl_3$, 500 MHz) δ (ppm) 5.34 (d, 1H, J=4.9 Hz), 3.69–3.64 (m, 10H), 3.39 (t, 2H, J=4.9 Hz), 3.22–3.15 (m, 1H), 2.40–2.34 (m, 1H), 2.25–2.18 (m, 1H), 2.04–1.01 (m, 26), 0.99 (s, 3H), 0.91 (d, 3H, J=6.3 Hz), 0.86 (dd, 6H, J_1= 6.3 Hz, J_2=2.2 Hz), 0.67 (s, 3H); ^{13}C NMR ($CDCl_3$, 125 MHz) δ (ppm) 140.9, 121.5, 79.4, 70.9, 70.7, 70.6, 70.0, 67.3, 56.7, 56.1, 50.6, 50.1, 42.3, 39.7, 39.5, 39.0, 37.2, 36.8, 36.1, 35.7, 31.9, 31.8, 28.3, 28.2, 28.0, 24.2, 23.8, 22.8, 22.5, 21.0, 19.3, 18.7, 11.8.

Synthesis of 8-(cholest-5-en-3β-yloxy)-3,6-dioxaoctanyl alendronate (ALN-TEG-Chol; compound 8)

8-(Cholest-5-en-3β-yloxy)-3,6-dioxaoctanyl azide (120 mg, 0.22 mmol) and 4.05 g (80 mg, 0.2 mmol) 1-hydroxy-4-pent-4-ynamidobutane-1,1-diyldiphosphonic acid were dissolved in tetrahydrofuran (THF)/methanol (MeOH)/water (1:1:1, v/v, 2 mL). $CuSO_4.5H_2O$ (5 mg, 0.02 mmol) and stabilizing agent (THPTA, 8.7 mg, 0.02 mmol) were dissolved in 0.5 ml THF/MeOH/water (1:1:1, v/v,), then sodium ascorbate (40 mg, 0.2 mmol) in 0.5 mL THF/MeOH/water (1:1:1, v/v,), was slowly added into $CuSO_4$ solution under argon to produce the catalyst solution, which was finally added drop wise into the reaction solution under argon. The reaction mixture was allowed to stir for 3 d at room temperature and then precipitated into methanol for three times. To remove copper, a large excess of EDTA (triamine tetracetate, sodium salt, silica-supported) was then added to the THF/water (1:1, v/v) solution of the product, stirred for 1 h at room temperature, and then filtered. Yield: 67%. ^{1}H NMR ($CDCl_3$, 500 MHz, 80°C) δ (ppm) 8.32 (s, 1H), 5.83 (s, 1H), 5.03 (s, 2H), 4.41 (s, 2H), 4.18–4.10 (m, 8H), 3.87 (m, 1H), 3.66 (m, 1H), 3.48 (m, 1H), 3.16–1.65 (m, 26H), 1.52–1.48 (m, 6H), 1.38 (d, 6H, J=6.3 Hz), 1.23 (s, 3H); ^{13}C NMR ($CDCl_3$, 125 MHz, 80°C) δ (ppm) 140.9, 121.5, 79.4, 70.9, 70.7, 70.6, 70.0, 67.3, 56.7, 56.1, 50.6, 50.1, 42.3, 39.7, 39.5, 39.0, 37.2, 36.8, 36.1, 35.7, 31.9, 31.8, 28.3, 28.2, 28.0, 24.2, 23.8, 22.8, 22.5, 21.0, 19.3, 18.7, 11.8.

Preparation and Characterization of Biomineral-Binding Liposomes

For the preparation of biomineral-binding liposomes (BBL), egg PC (or DSPC), cholesterol and ALN-TEG-Chol were dissolved in chloroform/methanol (1:1) solution. The lipid solutions were transferred into a flask and dried by evaporation under nitrogen stream to form a thin lipid film. The film was then dried under vacuum for 4 h at 4°C and then hydrated with PBS. For the preparation of BBL loaded with a hydrophobic model drug, β–carotene was added into the lipid solution. For the preparation of BBL loaded with rhodamine B (a hydrophilic model drug) or oxacillin, they were dissolved in PBS and added in the hydration step as described above. Nonbinding liposomes (NBL) were prepared similarly as described above without the addition of ALN-TEG-Chol. All liposome solutions were extruded through a 100-nm polycarbonate membrane with an Avanti® Mini-Extruder under nitrogen at room temperature to obtain liposomes with desirable sizes. Subsequent centrifugation with 10,000 rpm and purification with PD-10 column were performed to remove unencapsulated drug. The liposomes are characterized by dynamic light scattering (DLS).

Thermodynamic and Storage Stability Studies of Biomineral-Binding Liposomes

To thermodynamically investigate the phase transition changes of BBL caused by the incorporation of ALN-TEG-Chol (see Table II), the excess heat capacity functions of BBL were measured with DSC. All liposomes and reference buffer employed in the experiment were previously degasified under vacuum (140 mbar) for 15 min. The sample cell containing 0.7 mL of liposomal solution and the reference cell filled with the same volume of buffer solution were heated from 2 to 70°C at a heating rate of 0.75°C/min. Three heating scans were performed for each analysis to confirm the reproducibility of all thermograms. Analysis of the resulting thermograms yielded standard thermodynamic profiles (ΔH_{cal}, ΔS_{cal}, and $\Delta G°_T$). These profiles were obtained from the following relationships, using procedures described

previously: $\Delta H_{cal}=\int \Delta C_p^a \, dT$ and $\Delta S_{cal}=\int (\Delta C_p^a/T) \, dT$, where ΔC_p^a represents the anomalous heat capacity during the phase transition. The free energy change at any temperature, $\Delta G°_T$, is obtained from the Gibbs equation: $\Delta G°_T=\Delta H_{cal} - T\Delta S_{cal}$. The van't Hoff enthalpies, ΔH_{vH}'s are determined from analysis of the shape of the experimental DSC curves using procedures described earlier (23).

For the stability study of BBL formulated with ALN-TEG-Chol, BBL with different lipid compositions (see Table II and Fig. 4) were tested. All liposomal samples (5 mg/mL) were prepared and sealed in glass vials filled with argon and kept in darkness at room temperature for visual observation and DLS analysis.

Binding Potential and Kinetics of Biomineral-Binding Liposomes on HA Particles

Hydrophilic model drug rhodamine B, hydrophobic model drug β–carotene, and antimicrobial oxacillin loaded liposomes were prepared using the method described above. For the binding potential study, hydroxyapatite (HA) was added into rhodamine B and β–carotene loaded liposomal solutions; and the mixtures were agitated for 30 min at room temperature. After filtration, washing with water, and lyophilization, HA particles were observed under a fluorescence microscope. For the binding kinetics study, HA (100 mg) was added into 1 mL of oxacillin-loaded liposomal solution. After the mixtures were agitated for 1, 3, 5, 10, 30 min separately at room temperature, HA was removed by centrifugation (7,000 rpm, 1 min), and 100 μL of the supernatant was collected and analyzed by HPLC: Agilent C_{18} reverse-phase column (4.6×250 mm, 5 μm); mobile phase, 0.02 M KH_2PO_4/acetonitrile/methanol (70:25:5, v/v) at a flow rate of 1 mL/min; UV detection at 225 nm. The amount of oxacillin that bound to HA particles via the liposomal formulation was calculated by subtracting the amount of oxacillin left in the liposomal supernatant after binding from the initial amount of oxacillin in liposomes before binding. Nonbinding liposomes without ALN-TEG-Chol were used as controls in these experiments.

In Vitro Oxacillin Release Study of Biomineral-Binding Liposomes

Liposomal formulations were sealed into a dialysis bag (MWCO 25,000 kDa) incubated in 30 mL of release medium (10 mM PBS, pH=7.4) to release the encapsulated oxacillin at 37°C with gentle stirring. At predetermined time intervals, samples (1 mL) were removed from the release medium and replaced with fresh medium. The collected samples were diluted, filtered (0.2 μm) and analyzed with HPLC using the method described above.

In Vitro inhibition of *S. Aureus* Biofilm Growth Using Oxacillin-Loaded Biomineral-Binding Liposomes

S. aureus UAMS-1, a commonly used clinical osteomyelitis isolate described previously (24) was used in the biofilm inhibition studies. Autoclaved HA discs were incubated with different treatment formulations and saline in a 24-well plate for 10 min and then washed with saline to remove unbound liposomes or drug. The HA discs were then transferred to wells containing 1 mL of *S. aureus* suspension (OD= 0.05 at 600 nm) in Trypticase Soy Broth (TSB) and cultured statically for 24 h at 37°C to allow biofilm development, prior to quantification of bacterial growth.

At the end of each experiment, HA disc biofilms were individually transferred to a well containing 1 mL of TSB medium. The surface of each HA disc was gently scraped with a sterile spatula to harvest adherent cells. The removed biofilms were subjected to vortex mixing for 10 s and then serially diluted in TSB medium at a 1:10 ratio. The number of viable cells in each sample was quantified using the track dilution method (25). All plates were incubated for 24 h at 37°C and then the CFUs recovered per biofilm were determined.

Statistical Analysis

Data is expressed as mean±SD. For the bacterial study, specific differences between the log-CFU/biofilm of each experimental group were analyzed using the Student *t*-test (Microsoft Office 2007, Excel). A p-value of <0.05 was considered as statistically significant.

RESULTS

Preparation and Characterization of Biomineral-Binding Liposomes

As stated above, one potential solution to bacterial infection during orthopedic surgery/implantation is to prevent bacterial colonization by loading the implant surface with antimicrobials. Different from the current approaches, we propose to develop an orthopedic implant binding liposome platform. To incorporate implant-binding capacity to the liposomal formulations, a novel cholesterol derivative was designed using alendronate (ALN) as the HA binding moiety. The versatile click reaction was used to conjugate the hydrophilic ALN and hydrophobic cholesterol. After ~100% tosylation of the cholesterol, it was then refluxed with excess of tri(ethyleneglycol) or TEG to undergo a S_N2 substitution in order to introduce the hydrophilic linker into cholesterol. The purified product (compound 3) was then modified to introduce an azide group into cholesterol

(compound 5). Each step of these reactions was very efficient and was achieved with quantitative conversion. To make ALN click ready, the acetylene group was introduced (Compound 7) through EDC/NHS coupling between pentynoic acid and ALN. These two fragments were then successfully conjugated together through copper (I)-catalyzed Huisgen 1, 3-dipolar cycloaddition between the azide and alkyne with high yield at room temperature (Compound 8). From ^{1}H NMR spectrum, emergence of the singlet peak of 1,2,3-triazole at 8.32 ppm verified the successful conjugation.

DLS analyses (Table I) indicated that the average size of the liposomes in all preparations was between 150 and 165 nm with a polydispersity index ~0.1 indicating that liposomes with a relative homogenous distribution were obtained.

Thermodynamic and Storage Stability Studies of Biomineral-Binding Liposomes

Liposomes formulated by DSPC alone or by DSPC/ALN-TEG-Chol mixtures, with increasing molar proportions of ALN-TEG-Chol were prepared by the extrusion method. With the increase of ALN-TEG-Chol's molar ratio in the BBL formulation (11.1–50 mol%, Table II), the phase transition of DSPC was widened and depressed gradually while the transition temperature and the enthalpy of the liposomal solution decreased (Fig. 3). The phase transition of each formulation took place through enthalpy-entropy compensations yielding formulations with similar thermodynamic stabilities (Table II). The key observation is that the addition of ALN-TEG-Chol decreased the cooperativity of the DSPC phase transition, i.e. the size of the cooperative unit, equal to $\Delta H_{vH}/\Delta H_{cal}$, is reduced dramatically from 65 to 22, which may explain the findings from the storage stability experiment described below.

In the storage stability experiment, liposomes incorporated with ALN-TEG-Chol showed enhanced stability at room temperature during the observation period of 30 days (Fig. 4). Preparation 1, which was formulated without ALN-TEG-Chol or cholesterol started to aggregate within 48 h; while Preparation 2~6, which was formulated with ALN-TEG-Chol or cholesterol remained stable visually. One month later, Preparation 4, which was formulated with 33.3% ALN-TEG-Chol, showed the best stability, while all other formulations including Preparation 6, which had 33.3% cholesterol incorporated, showed evidence of aggregation and lipid precipitation. This aggregation was later confirmed by DLS while the particle size of Preparation 4 remained constant dynamically.

Table I Composition and Characterization of the Liposomes

Liposomes	Molar ratios/% (LPC/Chol/ALN-TEG-Chol)	Particle Size (nm)	PDI	Zeta Potential (mV)
NBL	70/30/0	152.1 ± 0.8	0.12 ± 0.03	−30.4 ± 0.6
BBL	70/20/10	164.5 ± 1.3	0.13 ± 0.02	−58.4 ± 0.2

Table II Thermodynamic Profiles for the Phase Transition of DSPC as a Function of the Mole % of ALN-TEG-Chol[a]

Mole % of ALN-TEG-Chol in formulation	DSPC/ALN-TEG-Chol molar ratio	T_M (°C)	ΔH_{cal} (kcal/mol)	TΔS (kcal/mol)	$\Delta G°_{20}$ (kcal/mol)	ΔH_{vH} (kcal/mol)
0	10:0	54.8	8.8	7.9	0.9	572
11	8:1	51.8	6.7	6.0	0.7	302
20	4:1	50.5	6.5	5.9	0.6	290
33	2:1	47.1	4.1	3.8	0.3	102
50	1:1	42.8	3.0	2.8	0.2	65

[a] All DSC experiments were measured in distilled water. Experimental uncertainties are as follows: T_M (±0.5 °C), ΔH_{cal} (±3%), $T\Delta S_{cal}$ (±3%), $\Delta G°_{20}$ (±5%), and ΔH_{vH} (± 10%)

Binding Potential and Kinetics of Biomineral-Binding Liposomes on HA Particles

The hydrophilic model drug rhodamine B and the hydrophobic model drug β–carotene were incorporated into the aqueous core and the lipid bilayer of biomineral-binding liposomes (BBL) respectively to validate its loading versatility. After incubation with HA particles for 30 min, BBL loaded with rhodamine B or β–carotene showed strong binding ability to HA as determined by fluorescence

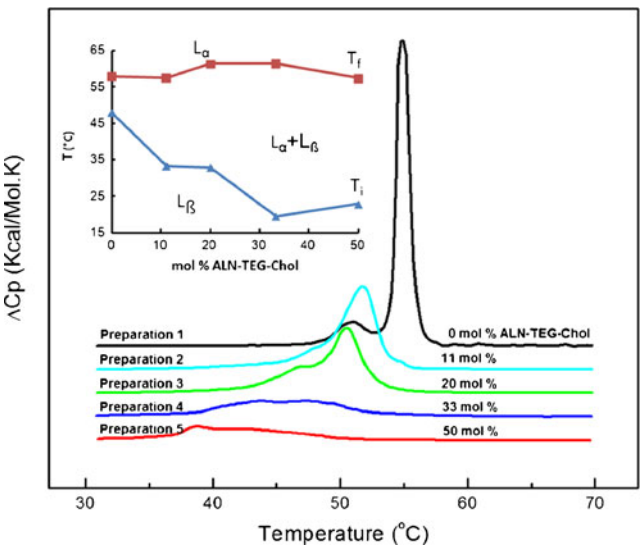

Fig. 3 DSC thermograms of BBL formulated with DSPC and ALN-TEG-Chol (5 mg/mL). Inset: phase diagram representing the initial (T_i) and final (T_f) temperature of phase transition. With increasing ALN-TEG-Chol concentration, there is a greater range where both phases coexist: gel phase (Lβ) and liquid-crystalline phase (Lα).

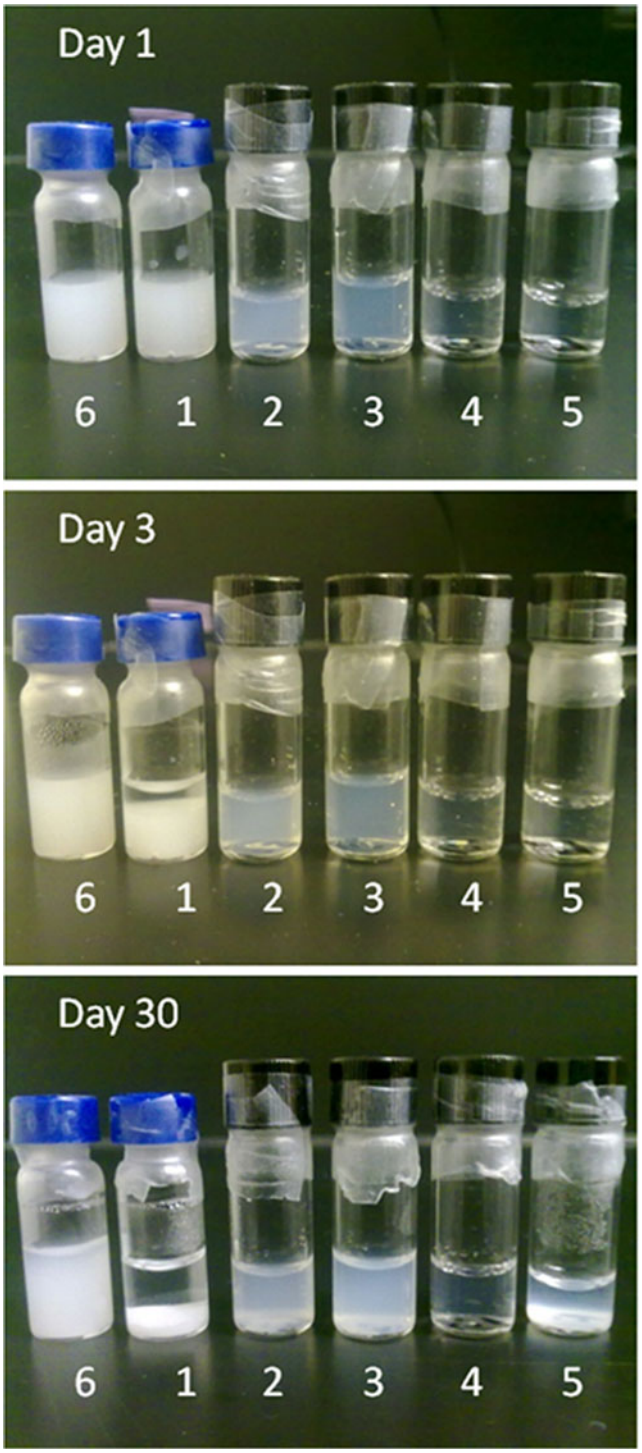

Fig. 4 Stability study of BBL formulated with DSPC and ALN-Chol. From left to right: Preparation 6 and 1∼5 which stand for 33 mole % of cholesterol, 0, 11, 20, 33 and 50 mole % of ALN-TEG-Chol in formulation respectively. All vials were sealed with argon inside and kept in dark at room temperature for visual observation.

microscopy when compared with the nonbinding control (Fig. 5). In the binding kinetics study (Fig. 6), most of the biomineral-binding liposomes loaded with oxacillin could swiftly bind to HA particles within 5 min and reach a binding plateau after 10 min (>70%). In the absence of ALN-TEG-Chol, the nonbinding liposomes demonstrated very limited non-specific binding to HA particles (<7%).

In Vitro Oxacillin Release Study of Biomineral-Binding Liposomes

The *in vitro* release profile of oxacillin from biomineral-binding liposomes that bound to HA particles was evaluated over a 24-h period. A large portion of the encapsulated oxacillin (65∼75%) was released from both biomineral-binding liposomes and the non-binding control within 6 h. The non-binding control had a slightly faster release rate than the biomineral-binding liposomes (Fig. 7).

In Vitro Inhibition of *S. Aureus* Biofilm Growth Using Oxacillin-Loaded Biomineral-Binding Liposomes

The results of the *in vitro* bacterial inhibition experiments (Fig. 8) indicated that the oxacillin-containing biomineral-binding liposomes (BBL) showed stronger inhibition of biofilm formation on HA discs when compared to the non-binding liposomes loaded with oxacillin (NBL), free drug (FD) and the other controls. Interestingly, free drug control also displayed a moderate, albeit significant inhibitory effect when compared to the other controls, which may result from the nonspecific binding of free oxacilin onto HA discs. The empty biomineral-binding liposomes (EBBL) without oxacillin loaded did not demonstrate any inhibition on biofilm formation. In summary, the inhibitory effect of oxacillin-containing BBL (4-log reduction in CFU/biofilm compared to untreated control, UC) was significantly higher than NBL (less than 1-log reduction in CFU/biofilm compared to UC).

DISCUSSION

The overall objective of this project was to develop a simple methodology to prevent osteomyelitis associated with orthopedic surgery and implantation. Different from the conventional implant surface modification or coating approaches, we believe that a novel implant-binding antimicrobial-loaded liposome formulation would provide surgeons with flexibility to personalize the prophylactic measures for infection in surgical implantation process. Liposomal formulation was selected as our working platform because of their long proven biocompatibility, versatility and most importantly the high potential for clinical translation (26,27). For its clinical application, we envision that surgeons will treat the implants with the novel liposomal formulations of different combinations (different antimicrobials, bone anabolic agents, etc.) in the OR prior to implant placement according to their clinical evaluation of the individual patient.

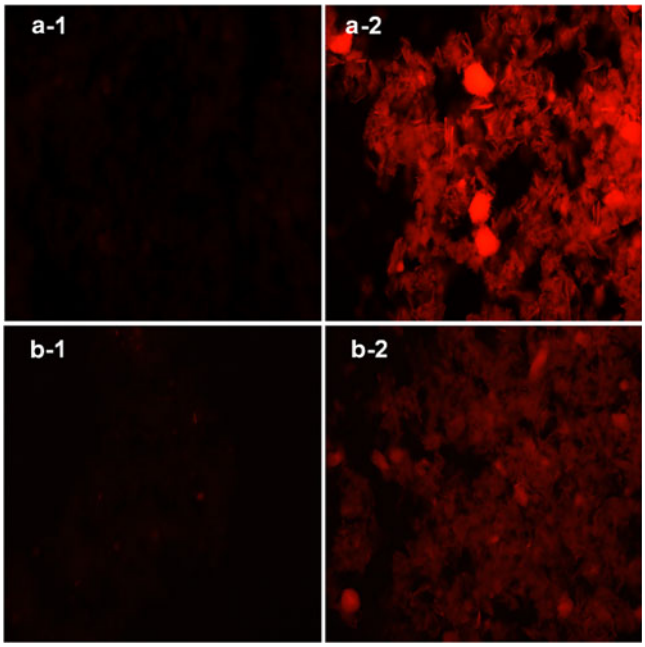

Fig. 5 Biomineral-binding ability of non-binding liposomes (a-1, b-1) and binding liposomes (a-2, b-2) loaded with rhodamine B (**a**) and β-carotene (**b**) on hydroxyapatite (HA) particles. Images were obtained on an Olympus BX51 microscope with an X-Cite® 120Q fluorescence microscopy illumination system, 100× magnification. One representative image out of six fields of view for each condition was selected.

As a proof of concept study, we chose to first develop a biomineral-binding liposome formulation, as many clinically used orthopedic implants were pre-coated with hydroxyapatite to promote osteointegration. Treating such implants with the novel liposomal formulation will provide a local antimicrobial barrier to prevent bacterial colonization. Even when they dissociate from the device surface during the implantation procedure, the liposomes may still anchor to the adjacent hard tissue, which would continue to contribute to the local antimicrobial concentration.

Cholesterol was selected as the molecule to introduce an implant-binding moiety, because it is a major component of the liposome lipid bilayer and the presence of a single secondary hydroxyl group in its structure provides the convenience for chemical modification (28). Alendronate (ALN) was selected as the biomineral-binding moiety to be conjugated to cholesterol. It belongs to a group of compounds called bisphosphonates (BPs), which are widely used clinically as anti-resorptive drugs for the treatment of osteoporosis. A unique feature of BPs is their strong binding ability to hydroxyapatite (HA) (29,30). As one of the most widely studied BPs, ALN has been used extensively as an osteotropic moiety for the development of bone-targeted drug delivery systems (22,31–33).

Though simple in its design, the direct conjugation of ALN (only soluble in basic aqueous solvent and limited solubility in acidic aqueous solvent) and cholesterol (very hydrophobic) was found to be extremely challenging. To solve this problem, Cu(I)-catalyzed Huisgen 1,3-dipolar cycloaddition of azides and alkynes was selected as the conjugation chemistry, which is one of the most frequently used "click" reactions for bioconjugation, polymer synthesis, and nanoparticle functionalization (17). It is characterized by mild reaction conditions (room temperature), good functional group compatibility, high reaction yields, simple workup, strong reliability, and most importantly for us, working very well both in organic and aqueous solvent systems (34,35).

To facilitate the "click" reaction, a hydrophilic linker TEG was first conjugated to cholesterol to increase its hydrophilicity and then functionalized with azide, which was then coupled with acetylene-modified ALN via the click

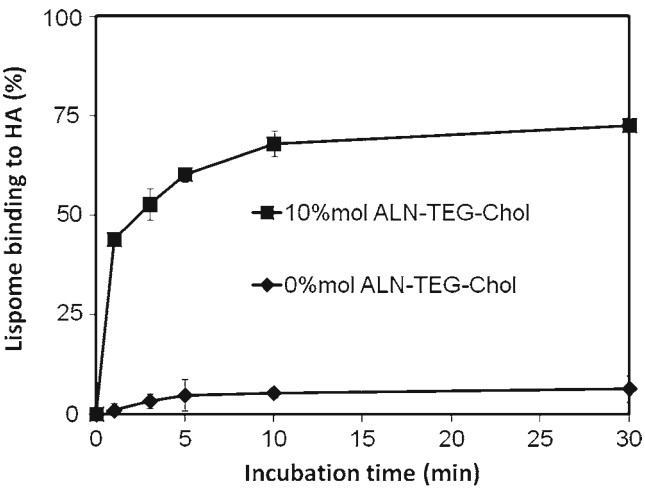

Fig. 6 *In vitro* binding kinetics of biomineral-binding liposomes (BBL) and nonbinding liposomes (NBL) on hydroxyapatite (HA) surface. All data are means ± standard deviations ($n=3$).

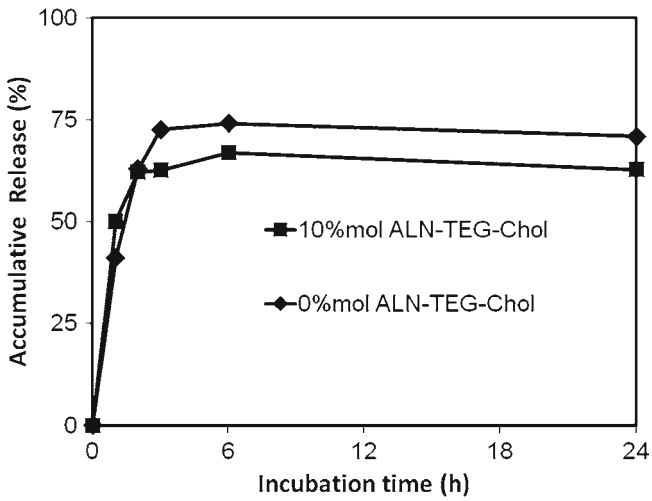

Fig. 7 *In vitro* oxacillin release study of biomineral-binding liposomes (BBL) and non-binding liposomes (NBL). All data are means ± standard deviations ($n=3$).

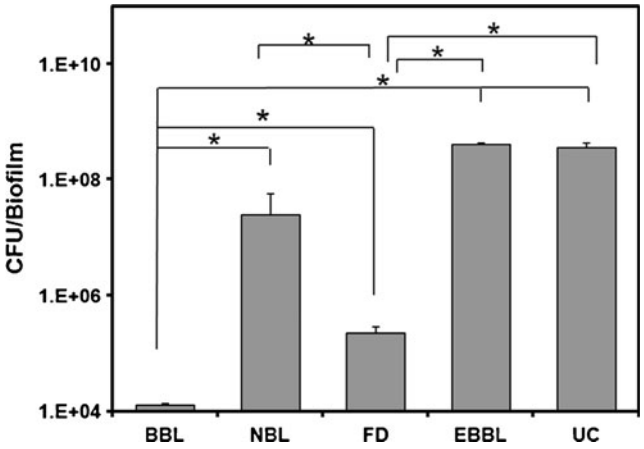

Fig. 8 Average number of CFU of *S. aureus* covered per hydroxyapatite (HA) disc after 24 h of incubation. HA discs were pretreated with the following formulations: biomineral-binding liposomes (BBL) loaded with oxacillin; non-binding liposomes loaded with oxacillin (NBL); free drug (FD, containing same amount of oxacillin as BBL or NBL); empty biomineral-binding liposomes (EBBL); and untreated control (UC). * $P < 0.0001$ (Student *t*-test). All data are expressed as means ± standard deviations ($n=3$).

reaction to obtain the biomineral-binding lipid ALN-TEG-Chol. This reaction was found to work very well in a mixed solvent system of THF/MeOH/H_2O and yields the target compound with high convention ratio (~100%). It is very important to emphasize that different from several other groups' approaches to introduce BPs onto liposome surfaces (36–38), which were designed exclusively for BP conjugation, the use of "click" chemistry would allow the incorporation of other metal binding moieties to be incorporated via the same chemistry scheme.

From the data generated by the DLS analysis, BBL and NBL were found to be similar in particle size and size distribution (~150 nm, PDI=0.1), suggesting the incorporation of ALN-TEG-Chol instead of cholesterol did not induce any significant change in the physicochemical properties of the liposome formulation.

One of the major effects of cholesterol incorporation into the phospholipid bilayer is the broadening and eventual elimination of the cooperative gel-to-liquid crystalline phase transition, replacing it with a phase having an intermediate degree of organization (39). This new organization results in altered membrane fluidity, increased mechanical strength, and decreased permeability (28). As the DSC data shows, the presence of ALN-TEG-Chol in the lipid mixture induced significant changes in the thermodynamic behavior of the liposomes. The broadening and depression of the phase transition peak lead to a reduction in calorimetric enthalpy (ΔH) (Fig. 3 and Table II) which ALN-TEG-Chol molar ratio was raised. The broadening of these peaks occurs due to a decrease of the phase transition cooperativity caused by the presence of high concentrations of ALN-TEG-Chol. Similar to cholesterol, the DSC data demonstrated that with the increase of ALN-TEG-Chol concentration, there is a greater range in temperature where both gel phase and liquid-crystalline phase coexisted (Fig. 3), i. e, significant broadening of the transitions. Moreover, we also observed a decrease in the magnitude of the enthalpy-entropy compensations with the increase of ALN-TEG-Chol concentration in the liposomes (Table II), suggesting that this biomineral-binding lipid also makes the lipid systems more fluid by affecting lipid-lipid interactions as reported previously in the case of the unmodified cholesterol (40). In addition to the similar abilities of unmodified cholesterol and ALN-TEG-Chol in regulating the phase behavior and integrity of the liposomal membranes, the negative charge on the polar end of the ALN-TEG-Chol molecule could further increase liposome stability by preventing BBL aggregation due to the electrostatic repulsion. This might explain the enhanced stability of the BBL incorporated with ALN-TEG-Chol when compared to the control containing similar amounts of cholesterol.

The data from the binding potential and kinetics studies reveal that BBL exhibits a strong affinity and rapid binding rate to biomineral material (Figs. 5 and 6). With these binding kinetics, its loading onto the orthopedic implant can be easily adapted in the OR setting as a part of the pre-implantation preparation protocol. The oxacillin containing liposome was observed with a fast release profile (Fig. 7). For the clinical setting of orthopedic device implantation, the first several hours at/post surgery is the opportune window for bacterial colonization and biofilm formation on the implant surfaces (7). An initial fast and steady release of a high dose of antimicrobials from the device surface could sufficiently reduce the likelihood of bacterial colonization and biofilm formation; ultimately improve the prophylaxis against infection and accelerate the patients' recovery (11).

The *in vitro S. aureus* biofilm growth inhibition assay (Fig. 8) confirmed the potential benefits as the BBL delivery system. The results demonstrated that the HA surface (representing the device coated with HA for better osteointegration) loaded with oxacillin-containing BBL could dramatically improve the protection against *S. aureus* colonization and biofilm formation when compared to NBL, FD and EBBL (at minimum of 1 order of magnitude). To understand the moderate inhibition of bacterial growth caused by free drug, we evaluated the non-specific binding of oxacillin to HA surface. It was found that 9.37 ±1.54% ($n=3$) of oxacillin was bound to the surface of HA disc after incubation (10 min) and repeated washing. The presence of three neighboring carbonyl groups offers potential sites for Ca^{2+} chelation and HA binding, which may explain the significant non-specific binding of oxacillin to the HA surface. *In vivo* studies using animal models that mimic the

clinical orthopedic device implantation setting are needed to further validate advantages of the antimicrobial-containing BBL delivery system.

The evolution of drug-resistant bacterial strains has plagued the clinical use of antibiotics. The β-lactamase-resistant penicillins (methicillin, oxacillin etc.) were developed to treat penicillin-resistant *S. aureus*. However, methicillin-resistant *Staphylococcus aureus* (MRSA) has emerged and undergone rapid evolutionary changes and epidemiologic expansion to become a major cause of nosocomial and community associated infections worldwide (41). First-line treatment for serious invasive infections due to MRSA is mostly performed with glycopeptide antibiotics, such as vancomycin. To potentiate the prevention and treatment of orthopedic device associated osteomyelitis due to MRSA, we are currently formulating biomineral-binding liposomes containing vancomycin, which does not have the unique HA-binding capability of oxacillin.

CONCLUSION

In this proof of concept study, we have successfully developed a novel biomineral-binding liposome formulation for the prevention of orthopaedic implant associated osteomyelitis. As the major formulation excipient, the alendronate-based binding moiety was conjugated to cholesterol via the Cu(I)-catalyzed "click" reaction. The drug-containing liposome formulated with modified cholesterol demonstrates strong and fast binding capability to a model implant surface (hydroxyapatite disk). When challenged with a clinical *Staphylococcus aureus* isolate, the biomineral-binding liposome formulation of oxacillin demonstrated significantly better bacterial colonization prevention efficacy than all the controls. When other binding moieties and antimicrobials are employed, the success of this novel formulation platform may be effectively extrapolated for the prevention of orthopedic implant-associated infections caused by different bacterial pathogens and using different implant materials. Due to the versatile design of the system and the outstanding *in vitro* testing efficacy, this novel approach holds promise for reducing the frequency of implantable device-related infections.

ACKNOWLEDGMENTS AND DISCLOSURES

This work was supported in part by NIH grants R01 AI038901 (KWB), P01 AI83211 (KWB), R01 AR053325 (DW), a NSF grant MCB-1122029 (LAM) and an Innovation Grant from UNeMed Corporation (DW).

REFERENCES

1. Wu P, Grainger DW. Drug/device combinations for local drug therapies and infection prophylaxis. Biomaterials. 2006;27:2450–67.
2. Harris LG, Richards RG. Staphylococci and implant surfaces: a review. Injury. 2006;37 Suppl 2:S3–14.
3. Mader JT, Landon GC, Calhoun J. Antimicrobial treatment of osteomyelitis. Clin Orthop Relat Res. 1993;87–95.
4. Ostermann PA, Henry SL, Seligson D. Timing of wound closure in severe compound fractures. Orthopedics. 1994;17:397–9.
5. Price JS, Tencer AF, Arm DM, Bohach GA. Controlled release of antibiotics from coated orthopedic implants. J Biomed Mater Res. 1996;30:281–6.
6. Seligson D, Klemm K. Adult posttraumatic osteomyelitis of the tibial diaphysis of the tibial shaft. Clin Orthop Relat Res. 1999;30–6.
7. Hetrick EM, Schoenfisch MH. Reducing implant-related infections: active release strategies. Chem Soc Rev. 2006;35:780–9.
8. Kurtz SM, Lau E, Schmier J, Ong KL, Zhao K, Parvizi J. Infection burden for hip and knee arthroplasty in the United States. J Arthroplasty. 2008;23:984–91.
9. Bozic KJ, Kurtz SM, Lau E, Ong K, Vail TP, Berry DJ. The epidemiology of revision total hip arthroplasty in the United States. J Bone Joint Surg Am. 2009;91:128–33.
10. Lew DP, Waldvogel FA. Osteomyelitis. N Engl J Med. 1997;336:999–1007.
11. Diaz-Rodriguez P, Landin M, Rey-Rico A, Couceiro J, Coenye T, Gonzalez P, *et al.* Bio-inspired porous SiC ceramics loaded with vancomycin for preventing MRSA infections. J Mater Sci Mater Med. 22:339–47.
12. El-Husseiny M, Patel S, MacFarlane RJ, Haddad FS. Biodegradable antibiotic delivery systems. J Bone Joint Surg Br. 93:151–7.
13. Tanaka KS, Houghton TJ, Kang T, Dietrich E, Delorme D, Ferreira SS, *et al.* Bisphosphonated fluoroquinolone esters as osteotropic prodrugs for the prevention of osteomyelitis. Bioorg Med Chem. 2008;16:9217–29.
14. Takahashi T, Yokogawa K, Sakura N, Nomura M, Kobayashi S, Miyamoto K. Bone-targeting of quinolones conjugated with an acidic oligopeptide. Pharm Res. 2008;25:2881–8.
15. Schmidmaier G, Lucke M, Wildemann B, Haas NP, Raschke M. Prophylaxis and treatment of implant-related infections by antibiotic-coated implants: a review. Injury. 2006;37 Suppl 2: S105–12.
16. Bernthal NM, Stavrakis AI, Billi F, Cho JS, Kremen TJ, Simon SI, *et al.* A mouse model of post-arthroplasty Staphylococcus aureus joint infection to evaluate *in vivo* the efficacy of antimicrobial implant coatings. PLoS One.5:e12580.
17. Hein CD, Liu XM, Wang D. Click chemistry, a powerful tool for pharmaceutical sciences. Pharm Res. 2008;25:2216–30.
18. Khoo X, O'Toole GA, Nair SA, Snyder BD, Kenan DJ, Grinstaff MW. Staphylococcus aureus resistance on titanium coated with multivalent PEGylated-peptides. Biomaterials. 31:9285–92.
19. Yoshinari M, Kato T, Matsuzaka K, Hayakawa T, Shiba K. Prevention of biofilm formation on titanium surfaces modified with conjugated molecules comprised of antimicrobial and titanium-binding peptides. Biofouling. 26:103–10.
20. Kumar V, Abbas AK, Fausto N, Mitchell RN. Robbins Basic Pathology. 8th ed. Saunders Elsevier; 2007. p. 810–811.
21. Liu XM, Lee HT, Reinhardt RA, Marky LA, Wang D. Novel biomineral-binding cyclodextrins for controlled drug delivery in the oral cavity. J Control Release. 2007;122:54–62.
22. Liu XM, Thakur A, Wang D. Efficient synthesis of linear multifunctional poly(ethylene glycol) by copper(I)-catalyzed Huisgen 1,3-dipolar cycloaddition. Biomacromolecules. 2007;8:2653–8.

23. Marky LA, Breslauer KJ. Calculating thermodynamic data for transitions of any molecularity from equilibrium melting curves. Biopolymers. 1987;26:1601–20.
24. Gillaspy AF, Hickmon SG, Skinner RA, Thomas JR, Nelson CL, Smeltzer MS. Role of the accessory gene regulator (agr) in pathogenesis of staphylococcal osteomyelitis. Infect Immun. 1995;63:3373–80.
25. Jett BD, Hatter KL, Huycke MM, Gilmore MS. Simplified agar plate method for quantifying viable bacteria. Biotechniques. 1997;23:648–50.
26. Abraham SA, Waterhouse DN, Mayer LD, Cullis PR, Madden TD, Bally MB. The liposomal formulation of doxorubicin. Methods Enzymol. 2005;391:71–97.
27. Gaitanis A, Staal S. Liposomal doxorubicin and nab-paclitaxel: nanoparticle cancer chemotherapy in current clinical use. Methods Mol Biol. 624:385–92.
28. Ohvo-Rekila H, Ramstedt B, Leppimaki P, Slotte JP. Cholesterol interactions with phospholipids in membranes. Prog Lipid Res. 2002;41:66–97.
29. Zhang S, Gangal G, Uludag H. 'Magic bullets' for bone diseases: progress in rational design of bone-seeking medicinal agents. Chem Soc Rev. 2007;36:507–31.
30. Wang D, Miller SC, Kopeček J. Targeted drug delivery for musculoskeletal diseases. Adv Drug Deliv Rev. 2005;57:935–7.
31. Pan H, Sima M, Kopečková P, Wu K, Gao S, Liu J, *et al.* Biodistribution and pharmacokinetic studies of bone-targeting N-(2-hydroxypropyl)methacrylamide copolymer-alendronate conjugates. Mol Pharm. 2008;5:548–58.
32. Wang D, Miller S, Sima M, Kopečková P, Kopeček J. Synthesis and evaluation of water-soluble polymeric bone-targeted drug delivery systems. Bioconjug Chem. 2003;14:853–9.
33. Liu XM, Wiswall AT, Rutledge JE, Akhter MP, Cullen DM, Reinhardt RA, *et al.* Osteotropic beta-cyclodextrin for local bone regeneration. Biomaterials. 2008;29:1686–92.
34. Kolb HC, Finn MG, Sharpless KB. Click Chemistry: Diverse Chemical Function from a Few Good Reactions. Angew Chem Int Ed Engl. 2001;40:2004–21.
35. Rostovtsev VV, Green LG, Fokin VV, Sharpless KB. A stepwise huisgen cycloaddition process: copper(I)-catalyzed regioselective "ligation" of azides and terminal alkynes. Angew Chem Int Ed Engl. 2002;41:2596–9.
36. Anada T, Takeda Y, Honda Y, Sakurai K, Suzuki O. Synthesis of calcium phosphate-binding liposome for drug delivery. Bioorg Med Chem Lett. 2009;19:4148–50.
37. Hengst V, Oussoren C, Kissel T, Storm G. Bone targeting potential of bisphosphonate-targeted liposomes. Preparation, characterization and hydroxyapatite binding *in vitro*. Int J Pharm. 2007;331:224–7.
38. Wang G, Babadagli ME, Uludag H. Bisphosphonate-derivatized liposomes to control drug release from collagen/hydroxyapatite scaffolds. Mol Pharm. 8:1025–34.
39. Bolean M, Simao AM, Favarin BZ, Millan JL, Ciancaglini P. The effect of cholesterol on the reconstitution of alkaline phosphatase into liposomes. Biophys Chem. 152:74–9.
40. Halling KK, Slotte JP. Membrane properties of plant sterols in phospholipid bilayers as determined by differential scanning calorimetry, resonance energy transfer and detergent-induced solubilization. Biochim Biophys Acta. 2004;1664:161–71.
41. Boucher H, Miller LG, Razonable RR. Serious infections caused by methicillin-resistant Staphylococcus aureus. Clin Infect Dis. 51 Suppl 2:S183–97.